A FE procedure for calculation of fixity of jack-up foundations with skirts using cyclic strain contour diagrams

H.P. Jostad*, Ø. Torgersrud and H.K. Engin
Norwegian Geotechnical Institute (NGI)

H. Hofstede
GustoMSC

* *corresponding author: hpj@ngi.no*

ABSTRACT

Foundation fixity or global soil spring stiffnesses plays an important role on dynamic behaviour and structural utilization of jack-up platforms, especially at large water depths. In order to establish accurate values for this fixity, one needs to account for the complex non-linear behaviour of the different soil layers involved under combined average and cyclic loading. A procedure for establishing non-linear stress-strain relationships to be used as input to finite element analyses of jack-up footings is presented. The calculated non-linear load-displacement relationships (foundation stiffnesses) of the individual footings are divided into cyclic and total (average plus cyclic) components to be used as input to the dynamic and quasi-static structural analyses of the jack-up. A realistic case, the GustoMSC AJ70 accommodation jack-up with 22 m diameter footings equipped with 2 m long skirts that penetrates into an overconsolidated clay at a water depth of 135 m in the North Sea is analysed. The obtained bearing capacity envelope and rotational stiffnesses are compared with corresponding results based on standard industry practice, ISO 19905-1.

KEY WORDS: jack-up, foundation stiffness, fixity, cyclic loading, skirts, finite element analyses, OC clay

INTRODUCTION

Jack-up rigs are widely used offshore as mobile drilling units for exploration and production of hydrocarbons, service platforms, accommodation platforms, etc. For a jack-up rig to be feasible in large water depths, it is often necessary to take moment fixity of the footings into account in order to reduce the critical moment in the lower leg guides, reducing the inertia forces (i.e. lower the natural period of the platform) and reducing the second order moment in the leg (p-Δ effect). The moment fixity may be increased by equipping the footings with skirts that penetrates into the soil. The effective embedment of the footings in stiff soils may then be increased significantly without increasing the preload. The achieved increased footing embedment compared to a standard spud-can will increase the bearing capacity and rotational stiffness of the footings.

However, since the static vertical bearing capacity of these footings are not defined, i.e. verified by the preload, but needs to be calculated (as for other types of offshore foundation), it is questioned whether the existing recommended practice for jack-up platforms [1] can be applied for non-penetrating footings with skirts or that additional guidance is needed to incorporate effects in this special case.

This paper presents a procedure for establishing non-linear stress-strain relationships from cyclic shear strain contour diagrams [2]. The procedure accounts for the complex behaviour of soil subjected to combined average and cyclic loading. A typical response from an undrained soil element test is presented in Figure 1. From this figure it is seen that the cyclic shear strain increases with increasing number of cycles (cyclic degradation). In addition, also the average or permanent shear strain increases with increasing number of cycles. The latter effect is important for the fixity of the footings under the peak storm loads due to the large average shear stresses

caused by the large average vertical loads combined with the average components of the local moment and horizontal load.

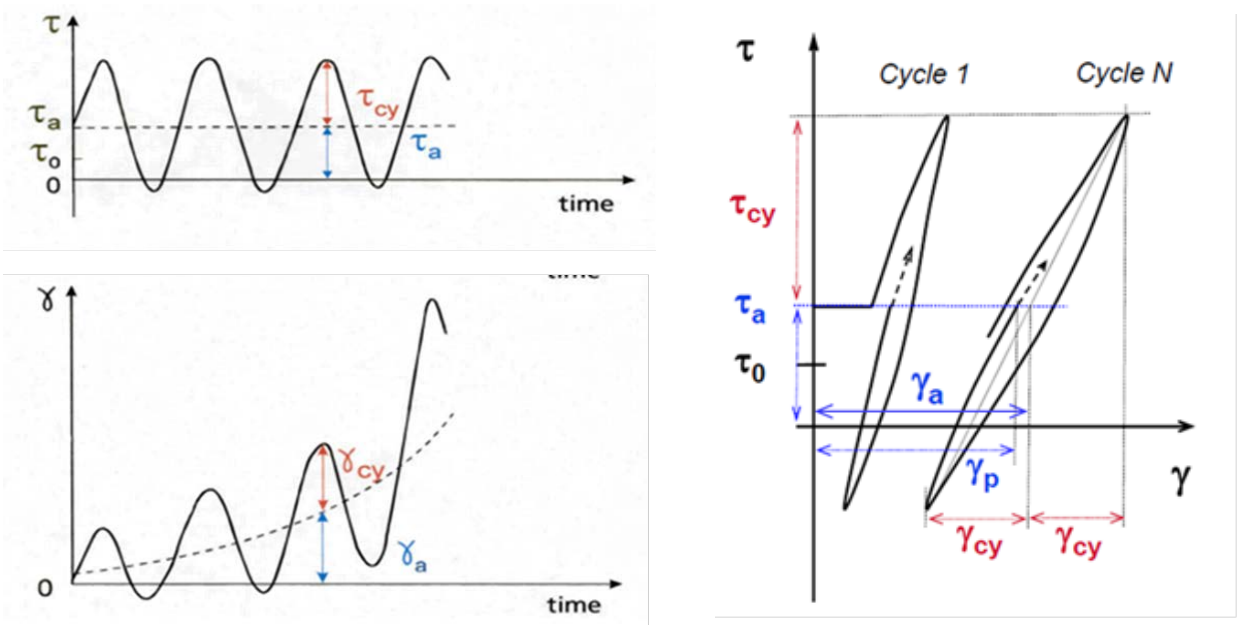

Figure 1 Development of average and cyclic shear strains with increasing number of cycles in a soil element subjected to combined average and cyclic shear stresses

NGI'S CALCULATION PROCEDURE

In this paper, NGI's procedure to account for cyclic loading is used to calculate the moment fixity of footings with skirts. The key ingredients in this calculation procedure are:

- Undrained average and cyclic shear stress – shear strain relationships as function of number of cycles obtained from 3D cyclic contour diagrams [2]. The diagrams are digitized by tables of sampling points (normalized average and cyclic shear stress τ_a/s_u and τ_{cy}/s_u, average and cyclic shear strain γ_a and γ_{cy}, and number of cycles N), and simple interpolation methods are used between these points. Here, average components are defined as the average value of the peak to trough values during a cycle. Correspondingly, the cyclic components are defined as the peak minus average value. This is also illustrated in Figure 1.
- The relationship between average and cyclic soil responses is found by two coupled FE analyses, where the average (or total) loads are applied in one analysis and the cyclic loads in the other analysis. This will for instance account for the important effect that the average shear strain may increase significantly due to cyclic loading.
- An equivalent number of cycles of the applied peak cyclic loads which represent the actual cyclic load history (design storm condition), is found by a strain accumulation procedure as described in [3].
- The undrained stress path (anisotropic) behaviour for a given material point is found by interpolation between triaxial (or biaxial) compression, extension and direct simple shear (DSS) type of undrained laboratory test behaviour.

This calculation procedure is for instance integrated in a material model called UDCAM [4]. In this paper a simplified version of the procedure is utilized. The approximations used in this simplified procedure are as follows:

- The equivalent number of cycles is calculated based on the design storm history of the normalized global overturning moment. The normalized shear stress history in all soil elements are assumed to be proportional (however with different scaling factors) to this global history. The equivalent number of cycles at failure (15% shear strain) is used for the stiffness calculations independent of the shear mobilisation of the actual material point.
- The ratio between the cyclic shear stress and average shear stress is based on the ratio between the cyclic and average global overturning moment of the jack-up platform during the largest wave in the actual design storm.

ISO PROCEDURE

The capacities and rotational stiffnesses obtained by NGI's procedure are compared with results obtained using the ISO 19905-1 approach [1].

It is noted that ISO standard 19905-1 has been developed with its basis founded in the Recommended Practice in SNAME T&R 5-5A Bulletin [5]. As such the ISO standard 19905-1 is written for use with pre-load verified foundations, such as for traditional spudcans, and not immediately for use in cases where the vertical capacity of the foundation, when determined by calculation based upon the defined strength profile of the given soil, is found to be in excess of the capacity that can be achieved by the pre-load. Nonetheless, the methodology as presently available in ISO Standard has been adopted here as if it were a pre-loaded foundation with the important deviation that the capacities have been calculated assuming full contact area.

EXAMPLE STUDY

The jack-up considered in this study is a GustoMSC AJ70 accommodation jack-up with footings being skirted spudcans with a base area of 380 m^2 each. External and internal skirts of 2 m length divide the spudcan into major compartments. Figure 2 shows a sketch of the example problem. For the calculations in this study, the footing is approximated as a flat circular base with D = 22 m, having outer skirts penetrating 2 m into the seabed and internal skirts preventing failure up between the skirts. The still water load, V_{SWL}, which is the vertical reaction load at seabed under normal operation (calm sea state) is assumed equal for all legs, V_{SWL} = 100 MN. The preload is equal to 160 MN.

The selected soil profile consists of a stiff clay with an overconsolidation ratio (OCR) of 40 in the top 7 m and an OCR of 4 below 7 m. The undrained shear strength is constant with depth and shown in Figure 3 together with the OCR profile. The profile shows the static undrained shear strength in triaxial compression, s_u^C. The anisotropic static shear strengths are s_u^{DSS} (direct simple shear) = 0.69 s_u^C and s_u^E (triaxial extension) = 0.56 s_u^C.

The small strain shear stiffness G_{max}, representing the initial, assumed elastic, stiffness of the soil is also shown in Figure 3. G_{max} can be measured in-situ offshore by use of seismic CPT or measured in lab tests on soil samples (resonant column, bender elements etc.). G_{max} can also be estimated by correlations with CPT cone resistance, relative density, undrained shear strength etc. However, site specific measurements of G_{max} are preferred when available. The G_{max} profile used in the NGI calculation in this paper is the low estimate design profile for the site, based on available measured data and correlations. In the ISO calculations, the formula given in ISO 19905-1 is used.

Static vertical bearing capacity

A Plaxis axi-symmetric model was used to calculate the static vertical bearing capacity of one footing. The NGI-ADP material model [6] was used to model the soil, using static anisotropic strength parameters. The vertical bearing capacity was calculated to V = 245 MN, which is higher than the preload of 160 MN. The footing base

is therefore expected to rest on the seabed after preloading. Full contact is assumed and, if needed, may be achieved by filling.

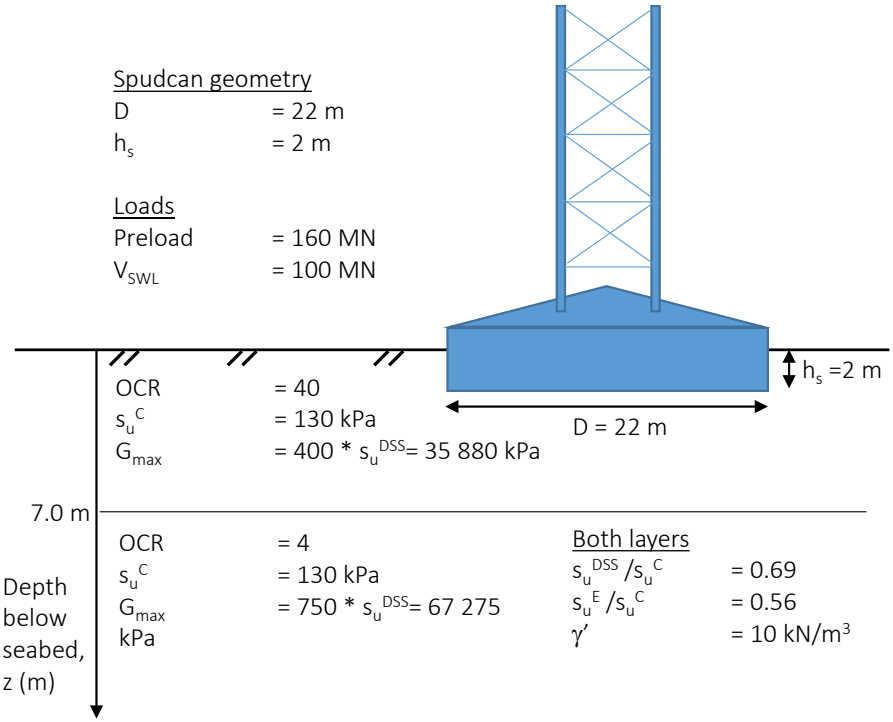

Figure 2 Basic properties of the example study

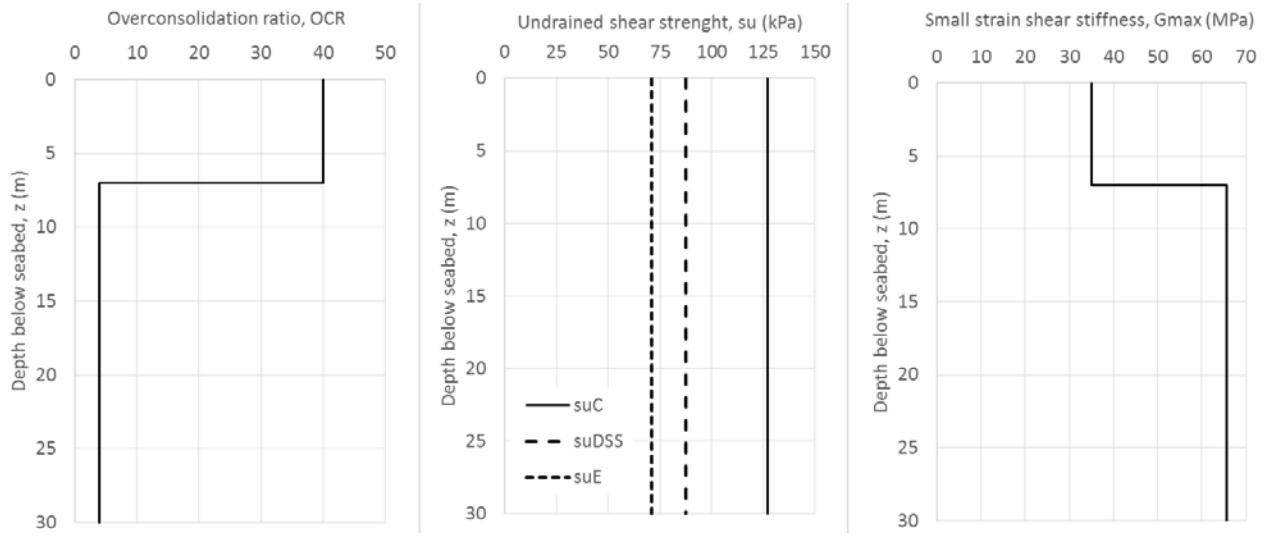

Figure 3 Overconsolidation ratio (OCR), undrained shear strength (s_u) and small strain shear stiffness (G_{max}) with depth

Cyclic stress-strain relationships

The cyclic load history at the footings during a design storm can be determined from dynamic wave analyses of the jack-up. In this example, the design storm is a 6-hour storm typically with a 100-year return period, and the

composition of the cyclic overturning moment (OTM) is shown in Table 1. The reaction moment is normalised with respect to the maximum cyclic OTM during the storm.

An equivalent number of cycles of the applied peak cyclic loads which represent the actual cyclic load history is found by the strain accumulation procedure [3]. Figure 4 shows the results from the strain accumulation procedure for the clay with OCR = 40 and OCR = 4. The shear strain contour diagrams were established from cyclic DSS tests. In the calculations, it was assumed that i) the cyclic shear stress history in the soil is proportional to the cyclic OTM, given in Table 1, and ii) the maximum cyclic shear stress gives failure in the soil element, where failure is defined as γ_{cy}=15 %. An equivalent number of cycles N_{eqv} at failure of 5 and 10 were found to be representative for OCR = 4 and OCR = 40, respectively.

Table 1 Composition of cyclic overturning moment (OTM) for a 6-hour design storm in the North Sea

Cyclic OTM in % of maximum	2	11	26	40	51	62	75	89	100
Number of cycles	2371	2877	1079	163	64	25	10	3	1

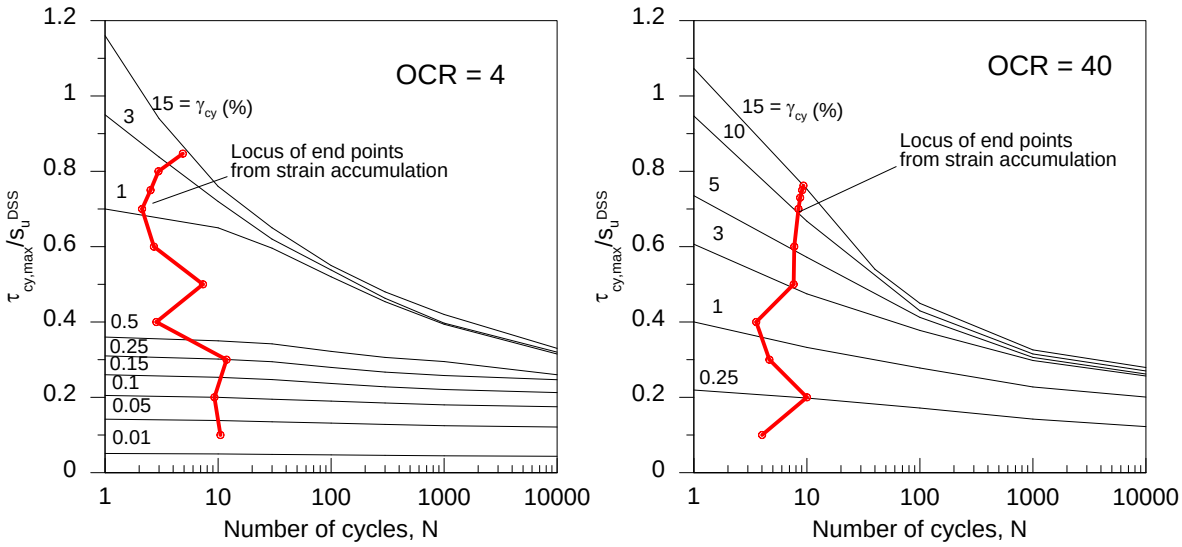

Figure 4 Results from strain accumulation procedure [3], giving N_{eqv} = 5 for OCR=4 and N_{eqv} = 10 for OCR=40

The cyclic shear stress – shear strain relationships for given idealized stress paths can now be obtained from the following;

1. Diagrams of cyclic and average shear strains (γ_{cy} and γ_a) as function of the normalized cyclic and average shear stresses (τ_{cy}/s_u and τ_a/s_u) for the calculated N_{eqv}.

2. Assumed shear stress ratios, i.e. the ratio between cyclic shear stress and average shear stress (τ_{cy} and τ_a) in DSS, triaxial extension and triaxial compression. The stress ratio in DSS was based on a superposition of the average shear stress mobilized due to the weight of the jack-up, and the ratio between cyclic and average shear stress due to the peak storm loading, OTM. The average shear stress mobilization under the weight of the jack-up was assumed as the ratio between the still water load and the static vertical bearing capacity; $\tau_{a,mob}/s_u^{DSS}$ = V_{swl} / V_{cap} = 100 MN / 245 MN = 0.41. The ratio between cyclic and average storm load components can be found from structural analyses of the jack-up. In this example the ratio between cyclic and average overturning moment, OTM = 3, was used. In

triaxial extension and compression, stress paths leading to similar shear strains (γ_{cy} and γ_a) as in DSS were assumed. The resulting idealized stress paths, starting from zero strains, are shown in the cyclic contour diagrams in Figure 5.

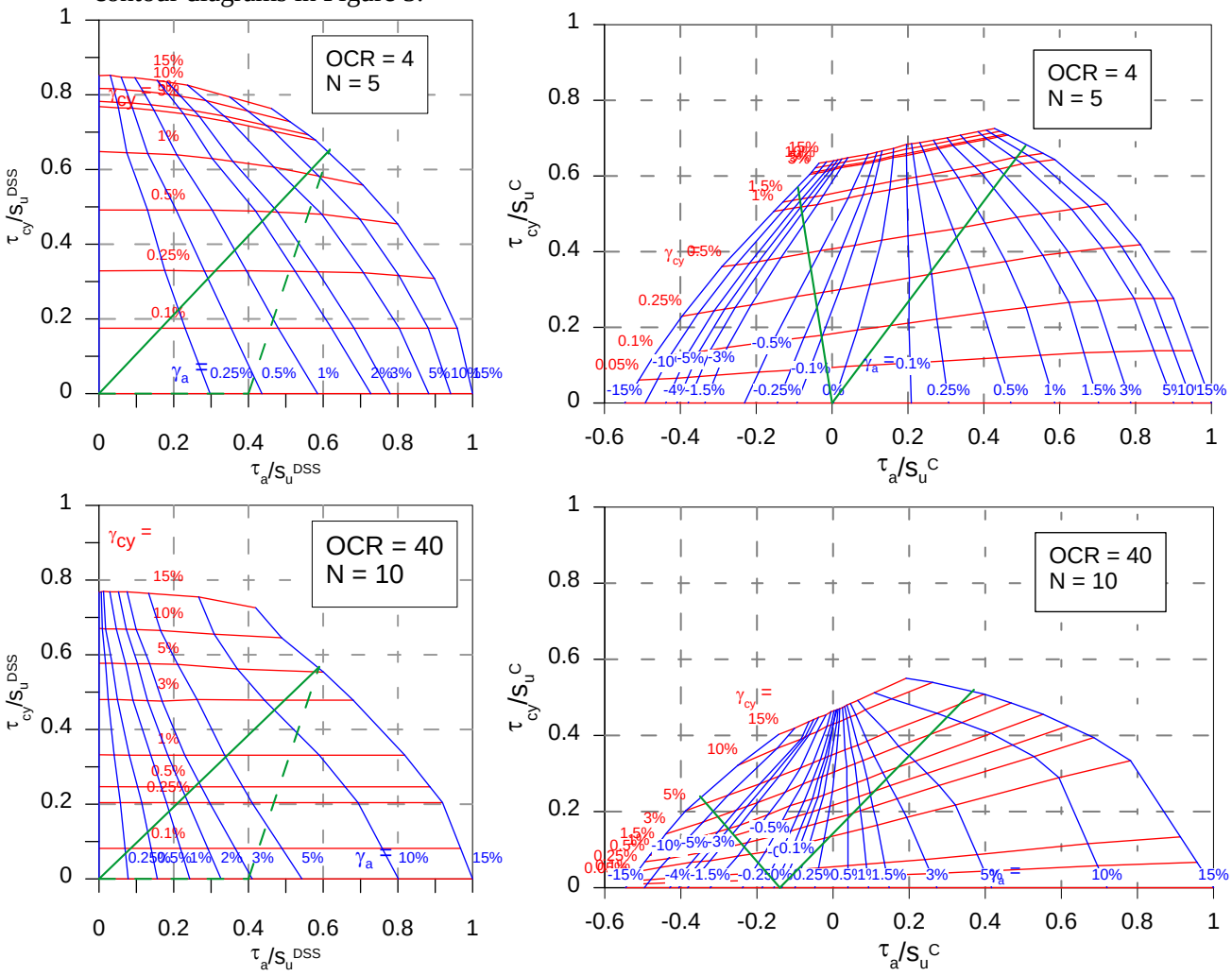

Figure 5 Cyclic contour diagrams for DSS and triaxial compression and extension, with selected stress paths

One can, by following the stress paths in the diagrams in Figure 5, establish shear stress-strain curves for cyclic loading (τ_{cy} - γ_{cy}), average loading, (τ_a - γ_a) and a combined cyclic and average loading as the sum of the two. In this example the following is calculated:

i) *Cyclic* foundation stiffness for use in *dynamic* jack-up analyses, based on cyclic shear-stress strain curves, see Figure 6.

ii) *Total* foundation stiffness for use in *quasi-static* jack-up analyses, based on the total shear stress – shear strain curves (sum of cyclic and average), see Figure 7.

As input to the finite element analyses the stress-strain curves are fitted to the non-linear hardening curve of the NGI-ADP model [6], shown in Figure 6 and Figure 7.

It is seen from the stress strain curves that the clay with OCR=40 is significantly more ductile than the clay with OCR=4. For OCR=40, the total secant shear modulus is reduced to less than 10% of G_{max} already at a shear stress mobilization of about 10% of s_u^{DSS}. For OCR=4, the corresponding shear modulus is significantly larger, i.e. 10% of G_{max} is reached first at a shear stress mobilization of about 50% of s_u^{DSS}. Furthermore, for both clays the cyclic stiffness is not significantly stiffer than the total stiffness.

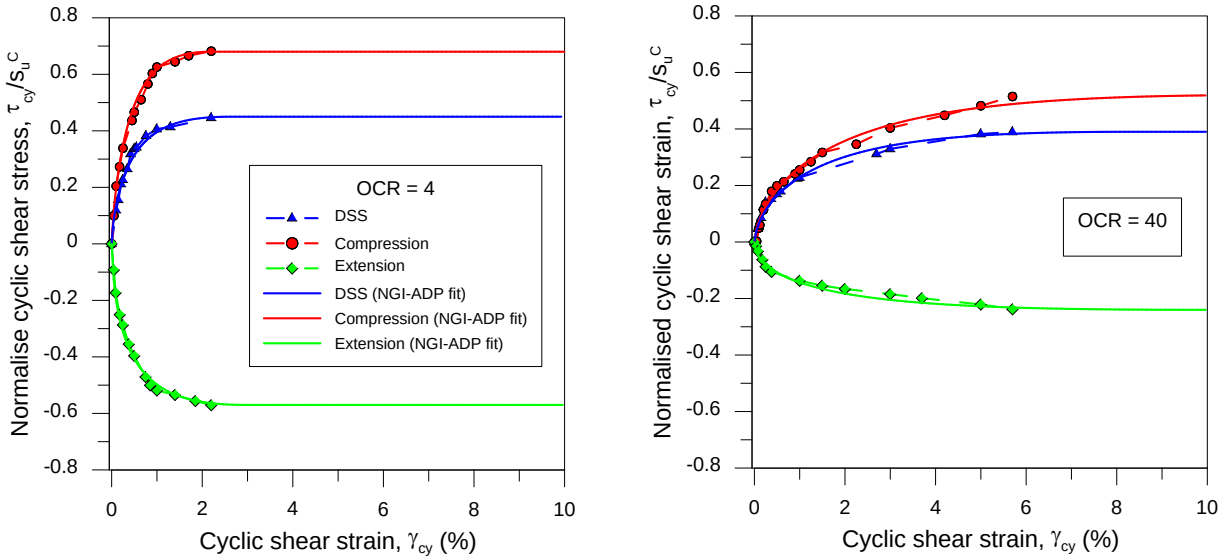

Figure 6 Cyclic shear stress – shear strain curves from contour diagram together with the NGI-ADP curve fits.

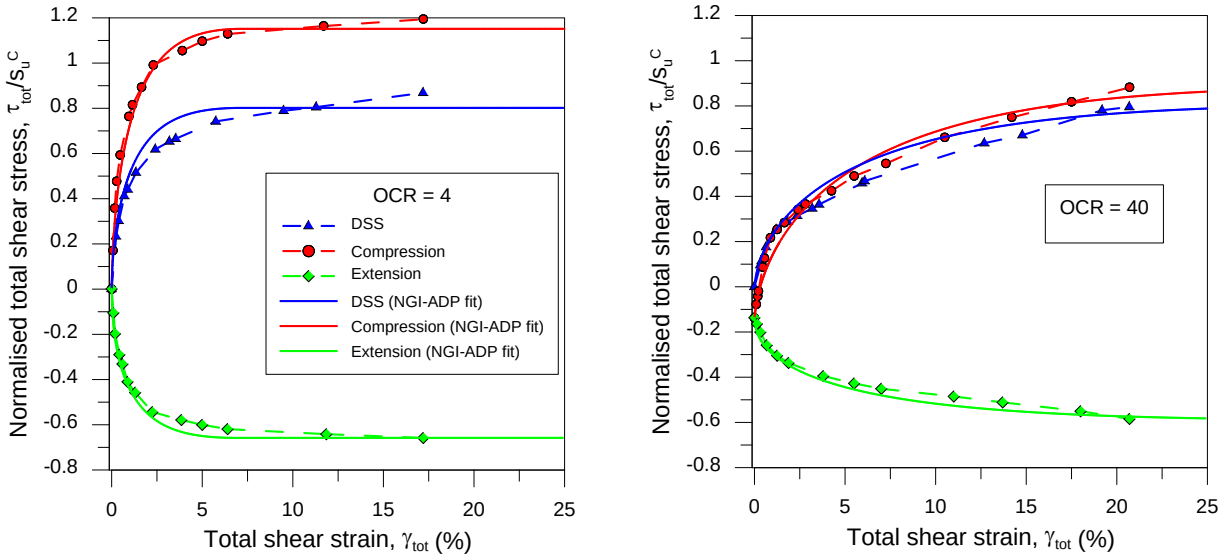

Figure 7 Total shear stress – shear strain curves from contour diagram together with the NGI-ADP curve fits

FE model for stiffness calculation

3D FEA were performed to calculate the footing foundation stiffnesses, using the commercial finite element software Plaxis 3D AE (www.plaxis.nl). The 3D model is shown in Figure 8. Due to symmetry along the centerline of the footing, a half of the footing and surrounding soil was modelled. The model consists of about 45000 10-noded tetrahedral soil elements, with an average element length in the refined failure zone of $L_{element}$ = 1.2 m. A mesh sensitivity study was performed with two finer mesh and shows that the maximum overshoot on capacity with the chosen mesh is about 10 %. It was not seen any significant overshoot on stiffness.

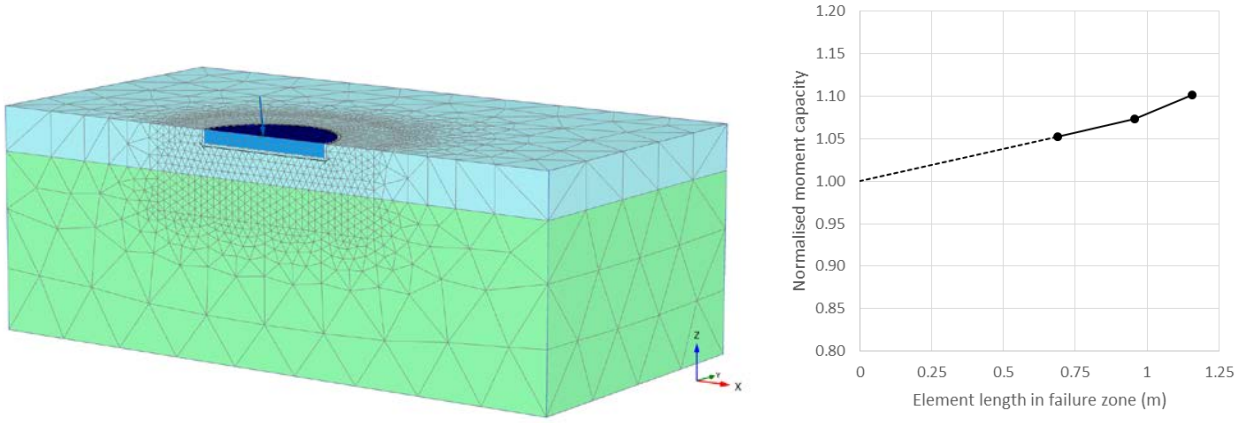

Figure 8 (a) FE-model for spudcan stiffness calculations. (b) Results from mesh sensitivity study, conservatively showing a 10 % overshoot on capacity with the chosen mesh (element length 1.2 m)

The clay was modelled as an undrained material using the material model called NGI-ADP [6]. This is a strain hardening elasto-plastic model with total stress path dependent anisotropic undrained shear stress – strain curves. The input to the model is the spatial distribution of the undrained active shear strength s_u^A, the anisotropy strength ratios s_u^{DSS}/s_u^A (direct simple shear, DSS) and s_u^P/s_u^A (passive), the corresponding shear shear strains at failure, γ_f^A, γ_f^{DSS} and γ_f^P, and initial elastic shear modulus ratio, G_o/s_u^A. Values for shear strength and failure strain parameters are taken from the stress-strain curves shown in Figure 6 and Figure 7. Please note that the internal strength parameters in the NGI-ADP are named s_u^A (s_u^C), s_u^{DSS} and s_u^P (s_u^E), however values used in this context are not the static strengths, but the cyclic and total strengths found from the contour diagrams. G_{max} is used as G_o. Separate analyses were performed for cyclic and total loads, with cyclic and total stress-strain curves respectively. The input parameters to the NGI-ADP model are summarized in Table 2 and Table 3.

The footing was modelled with 6-node plate elements and a high linear elastic stiffness to behave like a rigid body. Remoulding and set-up effect along the skirts was accounted for by use of interface elements with reduced strength equal to $0.3s_u^{DSS}$ [7].

Table 2 NGI-ADP parameters for cyclic FEA

	G_o/s_u^A	$s_u^A{}_{ref}$ (kPa)	s_u^{DSS}/s_u^A	s_u^P/s_u^A	τ_o/s_u^A	γ_f^C (%)	γ_f^{DSS} (%)	γ_f^E (%)	K_o'
Layer 1 (OCR = 40)	531	67.6	0.75	0.46	0.00	11.0	8.0	10.0	1.00
Layer 2 (OCR = 4)	761	88.4	0.66	0.84	0.00	2.0	2.5	2.0	1.00

Table 3 NGI-ADP parameters for total FEA

	G_o/s_u^A	$s_u^A{}_{ref}$ (kPa)	s_u^{DSS}/s_u^A	s_u^P/s_u^A	τ_o/s_u^A	γ_f^C (%)	γ_f^{DSS} (%)	γ_f^E (%)	K_o'
Layer 1 (OCR = 40)	313	114.6	0.90	0.67	-0.14	35.0	35.0	35.0	2.00
Layer 2 (OCR = 4)	450	149.5	0.70	0.57	0.00	7.0	7.0	7.0	1.00

Stiffnesses are calculated for the load range of interest. A horizontal load of 10 MN is assumed for all load cases, while the peak total vertical load is varying from 0 MN to 200 MN and a moment covering most of the range within the capacity envelope. The shear stress – shear strain curves used as input to the FEA represent the relation between stresses and strains accumulated and degraded through a whole storm. Therefore, in order to avoid any unrealistic history effects (other than included in N_{eqv}), each load case (V,H,M) is loaded up

proportionally from zero in the FE-model, and the rotational stiffness is taken as k_{rot} = M/rotation at the final load step of each calculation.

FE model for capacity calculations

Capacity envelopes for a footing subjected to combined cyclic and average loading were calculated from the in-house FE program HVMCap. The anisotropic cyclic undrained shear strengths used in the analyses are taken from Table 3. Description of the program may for instance be found in [8].

ISO stiffness and capacity envelope

The following procedure has been adopted:

- Calculate ultimate capacities (V,H,M) based on the average of the stress path dependent static undrained shear strength, full contact area and 2 m skirt penetration (embedment) using general capacity equations
- Estimate initial shear modulus (G) based on guidance for clay with OCR = 40 (Layer 1), not accounting for the stiffer clay layer (OCR=4) beneath 7 m depth
- Apply the non-linear rotational stiffness degradation model (with elastic translational springs) that accounts for the degradation of rotational stiffness (f_R) as a function of the foundation reactions (H,V,M) relative to the yield surface defined by the failure ratio r_f. By an iterative procedure, compatibility is achieved between rotation and moment reaction for all footings accounting for the non-linear soil stiffness and actual structural stiffness of the jack-up.

Table 4 summarizes the input parameters to the ISO assessment.

Table 4 Parameters used in ISO assessment of footing capacity and stiffness

s_u (kPa)	N_c (-)	R_{OC} (-)	$I= G_{max}/s_u$ (-)	α (-)	n (-)	γ_m (-)
97.5	6.3	40	238.6	1.0	1.0	1.0

The undrained shear strength is taken as the average of the s_u^C, s_u^{DSS}, s_u^E as defined in the soil profile. Full embedment and adhesion is assumed (α = 1). The stiffness reduction function f_R is based on n chosen as 1 in order to include the most conservative treatment of stiffness reduction [1], $f_R = 1 - r_f$. The selection of initial shear modulus G is based on A.9.3.4.3 of [1] with OCR = 40.

It is noted that the results of stage 1 (determine the dynamic amplification factor, DAF) is applied here as a quasi-static inertia load on the hull. The same inertia load set is applied in the ISO calculations as in the NGI calculations. More detailed investigations have been performed, a.o. through application of a kinematic hardening approach representing a non-linear foundation in time domain and compared to linear modelling and other methods for this specific condition in an accompanying paper [9].

It is also noted that despite the fact that the capacities and stiffnesses were based (indirectly) on soil strength, no additional material coefficient has been applied. It is assumed here that the same material coefficient would be needed also for the NGI procedure and, as such, the soil strength may be considered as a factored value. This is however not defined as part of the ISO Standard at the moment.

RESULTS AND COMPARISON WITH ISO 19905-1

Foundation capacity

The VM capacity envelope for a horizontal load equal to 10 MN is shown in Figure 9, together with capacity envelopes found using the ISO 19905-1 guidelines. It is observed from the NGI calculations that the pure vertical bearing capacity for a storm load (accounting for cyclic effects) becomes slightly higher than the static capacity (255 MN for H = 10 MN compared to 245 MN (H = 0). ISO gives a lower capacity of 233 MN (H = 0). Further, the shape of the VM capacity envelopes are comparable between the two methods. The NGI moment capacity is adjusted for windward legs (V < 100 MN) to account for that the crest of the cyclic component mobilise the soil more than the through. This is because the capacity diagram represent N_{eqv} number of the largest load, not only the peak state. The failure state is in this case governed by 15% average shear strain, including accumulated shear strains during the storm. The ratio between the maximum normalized momenent capacity M/D and maximum vertical capacity V is comparable (0.10 for ISO and 0.103 to 0.109 in NGI's surface).

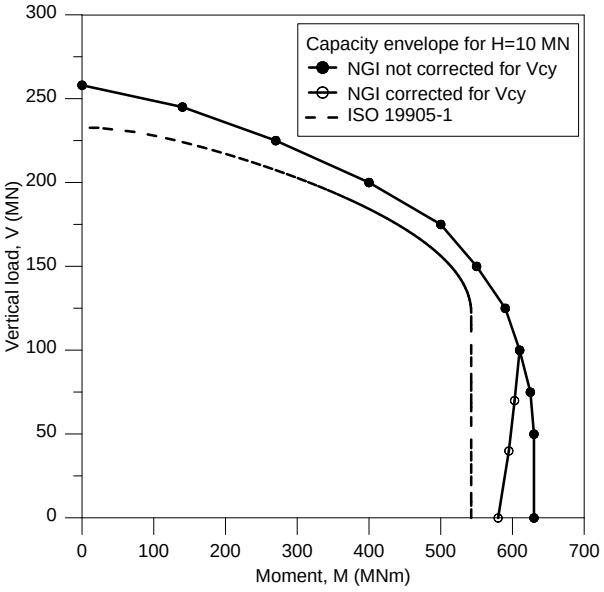

Figure 9 Foundation capacity as function of vertical and moment load for a horiozontal load of 10 MN

Foundation stiffness

Cyclic and total rotational stiffnesses as function of vertical load and moment are presented in Figure 10. The curves are for a horizontal load of H=10 MN and valid for a reference point at z = -2 m (skirt tip depth) which was found representative as the decoupling point where a horizontal load would give negligible rotation of the foundation. The total stiffnesses are secant values and valid for the actual combined cyclic and average storm loading of the foundation. Hence the stiffness accounts for accumulated deformations throughout the storm.

The initial small strain stiffness (based on G_{max}) is by the NGI procedure calculated to be 360 000 MNm/rad, while ISO gives a significantly lower value of 165 000 MNm/rad. This is mainly due to the lower G_{max}/s_u recommended in ISO, but also the difference by considering a two-layered soil in the FE-analyses compared to a homogeneous (with OCR=40) elastic halfspace solution in ISO.

The NGI cyclic rotation stiffness curves are comparable with the ISO curves but show a larger reduction in stiffness during increasing cyclic vertical load. They are however difficult to compare, since the ISO stiffness

curves are based on total capacities, not only the cyclic capacities. The NGI total rotation stiffness curves are significantly less stiff than the ISO curves. However, the stiffnesses are in this specific case relatively comparable in the range where compatibility with the structural stiffness occurs. The differences, especially at low moment, is discussed later in the paper.

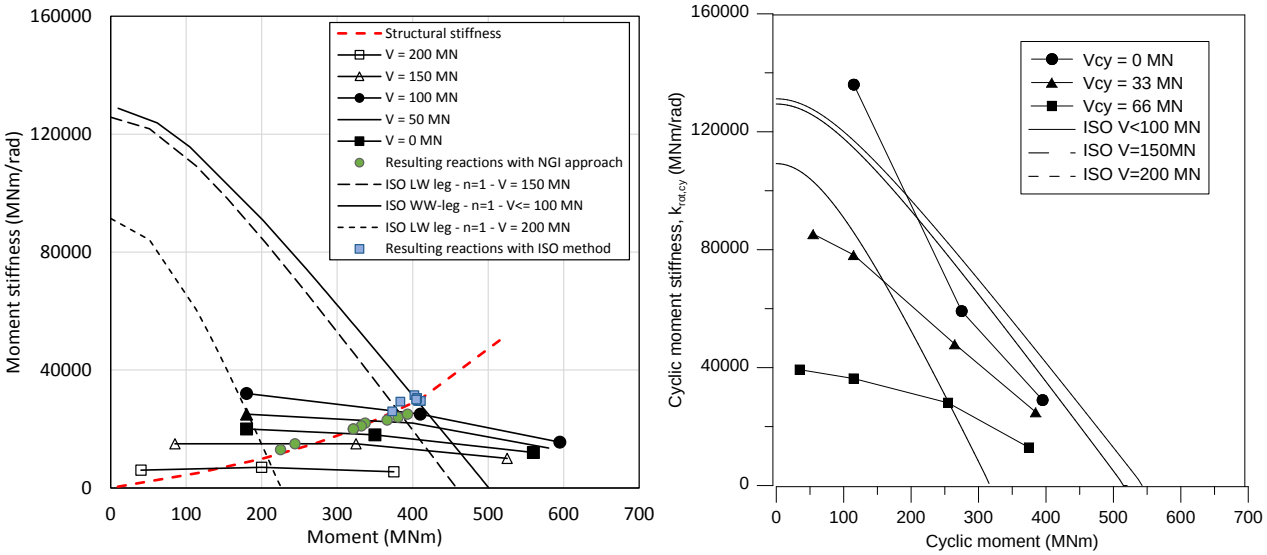

Figure 10 Total and cyclic rotational stiffnesses as function of total or cyclic footing moment and vertical load. The foundation stiffnesses are unfactored, i.e material factor equal to 1.0. ISO curves are with *n*=1 and do not destingush between cyclic or total loads

Structural response

The resulting foundation fixity have been translated into effects on the structural response and utilisation to indicate the relative effect of differences in resulting fixity. The resulting loads and fixities for 3 load headings are shown in Table 5 and Table 6. The structural utilisation as found with the fixity based on the NGI model is found as UC = 0.83. The resulting structural utilisation based on the ISO model is found as UC = 0.79.

Table 5 Resulting foundation fixities based on NGI stiffnesses

Load set heading	(deg)	240			210			180		
Leg		1	2	3	1	2	3	1	2	3
Horizontal reaction	(MN)	9.8	7.7	9.7	9.8	7.9	9.2	9.8	8.4	8.4
Vertical reaction	(MN)	65	159	76	46	151	103	39	131	130
Moment reaction	(MNm)	366	225	381	337	244	393	332	321	321
Rotational stiffness	(MNm/rad)	23000	13000	24000	22000	15000	25000	21000	20000	20000

Table 6 Resulting foundation fixities based on ISO stiffnesses

Load set heading	(deg)	240			210			180		
Leg		1	2	3	1	2	3	1	2	3
Horizontal reaction	(MN)	9.5	8.3	9.4	9.5	8.4	9.0	9.5	8.5	8.5
Vertical reaction	(MN)	68	154	78	51	146	103	44	128	128
Moment reaction	(MNm)	407	373	410	402	384	411	406	405	405
Rotational stiffness	(MNm/rad)	29500	26000	29500	31500	29250	29500	30500	30000	30000

DISCUSSIONS

The main difference between the total rotational stiffness curves obtained by the NGI approach and the curves derived from the equations in ISO 19905-1 is that the ISO formulation starts with the initial small strain stiffness at half the vertical bearing capacity or preload, (i.e. close to a typical operational load) and decreases more or less linearly (n=1) from this state toward failure, while the corresponding NGI stiffness curves are significantly lower especially at low moments.

The ISO formulation accounts for that the soil is in an unloading-reloading state after preloading which is assumed to give a very stiff response. In the present example the calculated bearing capacity (255 MN) is substantially higher than the defined pre-load (160 MN) and the effect of pre-loading on stiffness is then limited. Furthermore, the formulation neglect effects as cyclic degradation and accumulation of shear strains.

The NGI approach also accounts for the effect of a stiffer unloading/reloading stiffness when calculating the cyclic stiffness. The cyclic rotational stiffness curve starts from the small strain stiffness at the operational load and follows a nonlinear stiffness curve governed by the actual cyclic shear stress-shear strain relationship that accounts for the actual cyclic degradation. A typical effect of cyclic degradation was shown in Figure 1, where the cyclic stiffness decreases with increasing number of cycles.

Based on the actual cyclic shear stress-strain curves shown in Figure 7 for OCR=40, the secant shear modulus decreases very rapidly with increasing cyclic shear stress. For a cyclic shear stress that is only 10% of the undrained shear strength, the secant shear modulus is only about 10% of G_{max}. This explains why the cyclic rotational stiffness obtained by the NGI approach is lower at higher cyclic moments than obtained by the ISO formulations. This effect is significantly more pronounced due to the high over-consolidation ratio of 40 than compared to OCR = 4. The effect is demonstrated in Figure 11, where the rotational stiffness curves for a homogeneous clay with OCR=4 (and the same undrained shear strengths) are included. The results show that in this case NGI's method given higher rotational stiffnesses than the ISO method, i.e. 46500 MNm/rad (Leg 1), 35000 MNm/rad (Leg 2) and 46500 MNm/rad (Leg 3) for the load set heading of 240 degrees. These stiffnesses are in average 30% higher than the corresponding ISO curves.

The total stiffness curves obtained by the NGI approach are significantly lower than the ISO curves since based on the cyclic laboratory tests data (cyclic contour diagrams), there will be significant shear strain accumulations due to the high average shear stress mobilization under the actual large vertical loads. Although, also these curves should start at the initial small strain stiffness at the operational load, since there will be no strain accumulation when the cyclic loads are zero. But the curves drop significantly more rapidly than defined by the ISO degradation function.

Furthermore, in ISO it is assumed that the effect of preloading only gives a positive effect since the material then after unloading to the operational load is in an unloading/reloading state. However, for an over-consolidated clay the loading to large shear strains may remove some of the effect of the over-consolidation. This is for instance observed by disturbed samples were the pre-consolidation stress is lower than for a less disturbed sample. Loading to large shear strains may also break down part of the inherent structure of a natural clay.

For an overconsolidated clay one can also argue that the effect of preloading is already accounted for in the laboratory tests since the material already has been loaded up to the pre-consolidation stress. According to classical elastoplastic framework (e.g. the CamClay model), the anisotropically consolidated stress states used in the laboratory tests is already inside the virgin yield surface. It is also seen from the curves in Figure 6 and Figure 7 that the measured cyclic secant shear modulus for an overconsolidated clay is not significantly stiffer than the static secant shear modulus. However, it would have been interesting to check the effect of shearing the highly over-consolidated clay to large shear strains (preloading) before performing the cyclic tests.

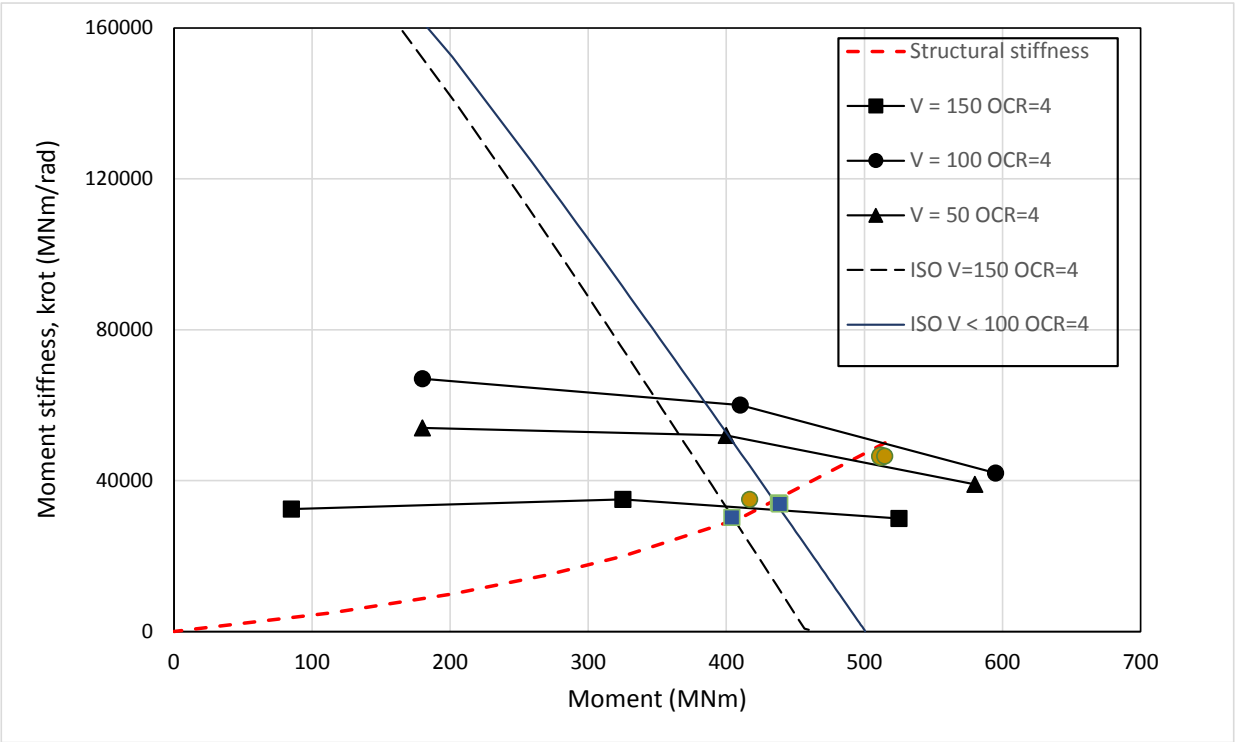

Figure 11 Total rotational stiffnesses as function of total footing moment and vertical load. The NGI's curves in Figure 10 are changed with calculated stiffnesses for a homogeneous clay with OCR=4 in order to demonstrate the effect of clay type

CONCLUSIONS

A finite element procedure for calculation of fixity of footings with skirts in clay during extreme storm loading is presented. The method accounts for the effects of combined average and cyclic loads, cyclic degradation of the cyclic stiffness, accumulation of permanent deformations which reduce the moment fixity, strain rate effects which increase the cyclic stiffness, and stress path (anisotropic) dependent undrained behaviour. The undrained shear stress-strain relationship is interpolated directly between anisotropically consolidated cyclic laboratory tests, instead of using a constitutive framework.

The method is applied to a realistic case, and the results are compared with results obtained using the standard industry practice given by ISO 19905-1. This is however a special case as the foundation capacity as calculated exceeds the pre-load (160 MN), yet treated as if the pre-load is virtually equal to the calculated capacity (233 MN).

The main conclusions from the paper are as follows:

- It is important to distinguish between cyclic foundation stiffnesses used in a dynamic structural analysis and the total foundation stiffnesses used to check the integrity of the jack-up in a quasi-static analysis.

- The non-linear foundation stiffness depends on the soil type. For instance, the secant stiffness at a given safety factor (load mobilization) is significantly lower for a highly overconsolidated clay (OCR=40) compared to a less overconsolidated clay (OCR=4). It is therefore important to account for the actual stress-strain relationships under combined average and cyclic loads for the soil layers involved. Better guidelines for selecting the degradation parameter n is therefore required. For highly overconsolidated

clays one may even need a formulation that gives a concave (up) degradation curve or alternatively a reduction on the initial shear modulus.

- The moment fixity under the peak loads may be highly affected by cyclic degradation and strain accumulation.

- Based on this example calculation, it is found that there is no guarantee that the fixities calculated by ISO 19905-1 are conservative especially for highly overconsolidated clays.

- For a homogenous clay with OCR=4, it is found that the NGI's method gives rotational stiffnesses that in average are about 30% higher than the corresponding ISO curves.

- In addition, it is recommended to perform some soil element tests to study the actual effects of initial undrained pre-loading to large strains followed by typical idealized cyclic load histories representative for typical storm loading of jack-up platforms.

REFERENCES

[1] International organisation for standardisation: Petroleum and offshore gas industries – site specific assessment of mobile offshore units – part 1: Jack-ups (ISO 19905-1:2012), Geneve, 2012.

[2] Andersen, K.H. 2015. Cyclic soil parameters for offshore foundation design. 3rd McClelland Lecture. Proc., Int. Symp. on Frontiers in Offshore Geotechnics, ISFOG, Oslo, Norway, June 2015.

[3] Andersen, K.H., Dyvik, R., Kikuchi, Y., Skomedal, E. (1992). Clay behaviour under irregular cyclic loading. Proc. 6th Int. Conf. on the Behaviour of Offshore Structures, London 2, 937-950

[4] Jostad, H.P. Grimstad, G., Andersen, K.H., Saue, M., Shin, Y. & You, D. 2014. A FE Procedure for Foundation Design of Offshore Structures – Applied to Study a Potential OWT Monopile Foundation in the Korean Western Sea. Geotechnical Engineering Journal of the SEAGS & AGSSEA, Vol. 45, No. 4.

[5] The Society of Naval Architects and Marine Engineers (SNAME). Guidelines for Site Specific Assessment of Mobile Jack-Up Units, August 2008

[6] Grimstad G., Andresen L., Jostad H.P. (2011). NGI-ADP: Anisotropic shear strength model for clay. International Journal for Numerical and Analytical Methods in Geomechanics, Vol. 36, No. 4, pp. 483-497.

[7] Andersen, K.H., and Jostad, H.P (2002). Shear Strength Along Outside Wall of Suction Anchors in Clay after Installation. Proceedings of the Twelfth ISOPE Conference, Kyushu, Japan, 26-31 May, 2002

[8] NGI (1997). BIFURC – Version 3. Undrained capacity analyses of clay. NGI Report nr 514052-1, dated 22 December 1997

[9] Hofstede, H., Hoogeveen, S.M., Skau, K., Torgersrud, Ø., Engin, H.K. Non-linear versus linear foundation modelling in dynamic response of an AJ70 jack-up. Proceedings of International Conference, The Jackup Platform, City University, London, 2015